

# Preparation, structures and physical properties of $\kappa$ -type two-dimensional conductors based on unsymmetrical extended tetrathiafulvalene: 2-cyclopentanylidene-1,3-dithiolo[4,5-*d*]-4,5-ethylenedithiotetrathiafulvalene (CPDTET)

Hideki Fujiwara,<sup>†a</sup> Yohji Misaki,<sup>\*a</sup> Masateru Taniguchi,<sup>a</sup> Tokio Yamabe,<sup>a</sup> Tadashi Kawamoto,<sup>b</sup> Takehiko Mori,<sup>b</sup> Hatsumi Mori<sup>c</sup> and Shoji Tanaka<sup>c</sup>

<sup>a</sup>Department of Molecular Engineering, Graduate School of Engineering, Kyoto University, Yoshida, Kyoto 606–8501, Japan

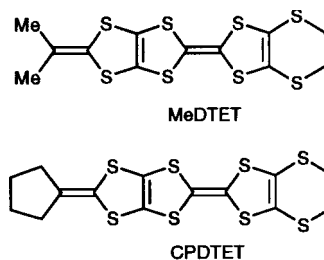
<sup>b</sup>Department of Organic and Polymeric Materials, Faculty of Engineering, Tokyo Institute of Technology, O-okayama, Tokyo 152–8552, Japan

<sup>c</sup>International Superconductivity Technology Center, Shinonome, Tokyo 135–0062, Japan

Several cation radical salts of an unsymmetrical donor, 2-cyclopentanylidene-1,3-dithiolo[4,5-*d*]-4,5'-ethylenedithiotetrathiafulvalene (CPDTET) have been prepared. Most salts with octahedral ( $\text{AsF}_6^-$ ,  $\text{SbF}_6^-$ ,  $\text{NbF}_6^-$  and  $\text{TaF}_6^-$ ) and linear ( $\text{I}_3^-$ ) anions showed high conductivity ( $\sigma_{\text{rt}} = 10^0\text{--}10^2 \text{ S cm}^{-1}$ ) and metallic conductive behaviour around room temperature. Among them, the  $\text{AsF}_6^-$  salt displayed metallic temperature dependence down to 4.2 K, while the  $\text{SbF}_6^-$  and  $\text{TaF}_6^-$  salts exhibited metal-to-semiconductor transitions at 200 and 140 K, respectively. The  $\text{AsF}_6^-$  and  $\text{SbF}_6^-$  salts have a  $\kappa$ -type donor arrangement in which two donor molecules are strongly dimerized in a 'head-to-head' manner. The calculated Fermi surfaces of these salts are two-dimensional folded circles. Measurement of the thermoelectric power suggests that the  $\text{AsF}_6^-$  salt is a normal metal, however, the  $\text{SbF}_6^-$  salt has an almost half-filled band structure at room temperature and a small energy gap opens at low temperature. The measurements of magnetic susceptibility indicate that these two salts exhibited Pauli-paramagnetic temperature independence characteristic of metallic materials, though they also showed weak antiferromagnetic interaction. The differences between  $\text{AsF}_6^-$  and  $\text{SbF}_6^-$  salts are also discussed and the origin of the metal-to-semiconductor transition is clarified.

In the search for new organic conductors the symmetrical TTF donors bis(ethylenedithio)-TTF (BEDT-TTF) and tetramethyltetraselenafulvalene (TMTSF) have played an important role and to date have yielded many superconductors.<sup>1,2</sup> On the other hand, the discovery of organic superconductors based on multisulfur unsymmetrical donors, methylenedithio-TTF (MDT-TTF)<sup>3</sup> and dimethylethylenedithio(dithiadiselenafulvalene) (DMET)<sup>4</sup> has greatly stimulated interest in preparing new classes of unsymmetrical TTF donors. In the course of exploring new substituents we have focused on the 1,3-dithiol-2-ylidene group as a promising substituent for realizing the two-dimensional arrangement of donor molecules required for stable organic metals.<sup>5</sup> Among newly synthesized TTF derivatives fused with 1,3-dithiol-2-ylidenes,<sup>5–7</sup> we have found that an unsymmetrical derivative 2-isopropylidene-1,3-dithiolo[4,5-*d*]-4,5'-ethylenedithio-TTF<sup>‡</sup> (MeDTET) has yielded several cation radical salts retaining metallic conductivity down to low temperature, and  $(\text{MeDTET})_3\text{PF}_6\text{TCE}_x$  has the so-called ' $\kappa$ -type' donor arrangement in the conducting sheet.<sup>8</sup> The realization of a  $\kappa$ -type structure has been recognized to be the most promising strategy for yielding new organic superconductors.<sup>9</sup> In this context, investigation of the physical properties of cation radical salts based on modified MeDTET derivatives is of considerable interest. In this article, we describe the preparation, crystal and electronic structures, transport and magnetic properties of cation radical salts of a MeDTET

analogue CPDTET, where CPDTET is 2-cyclopentanylidene-1,3-dithiolo[4,5-*d*]-4,5'-ethylenedithio-TTF.<sup>‡10</sup>



## Experimental

### Synthesis and electrocrystallization

CPDTET was prepared according to the literature,<sup>6b</sup> and was recrystallized from chlorobenzene before preparation of the cation radical salts. Single crystals of CPDTET salts were electrochemically grown in the presence of the corresponding tetra-*n*-butylammonium salts at a controlled current<sup>11</sup> of 0.2–0.5  $\mu\text{A}$  in chlorobenzene containing a small amount of EtOH (10%, v/v) at 25 °C for about two weeks. The  $\text{I}_3^-$  salt was obtained by mixing hot chlorobenzene solutions of the donor and tetra-*n*-butylammonium triiodide. Their compositions were determined by energy dispersion spectroscopy (EDS) from the ratio of sulfur and the elements designated in parentheses in Table 1, except for the  $\text{AsF}_6^-$  and  $\text{SbF}_6^-$  salts whose compositions were determined by X-ray crystal structure analysis.

<sup>†</sup>Present address: Institute for Molecular Science, Myodaiji, Okazaki 444–8585, Japan.

<sup>‡</sup>IUPAC names: 2-(5-isopropylidene[1,3]dithiolo[4,5-*d*]dithiol-2-ylidene)-5,6-dihydro[1,3]dithiolo[4,5-*b*][1,4]dithiine (MeDTET) and 2-(5-cyclopentylidene[1,3]dithiolo[4,5-*d*]dithiol-2-ylidene)-5,6-dihydro[1,3]dithiolo[4,5-*b*][1,4]dithiine (CPDTET).

**Table 1** Composition and electrical properties of CPDTET·(Anion)<sub>x</sub>

anion	$x^a$	$\sigma_{\text{rt}}/\text{S cm}^{-1}{}^b$	conducting behaviour
$\text{ClO}_4^-$	0.60 (Cl)	0.037	$E_a=0.15$ eV
$\text{PF}_6^-$	0.42 (P) <sup>c</sup>	0.015	$E_a=0.13$ eV
$\text{AsF}_6^-$	0.36 <sup>d</sup>	27	Metallic $\geq 4.2$ K
$\text{SbF}_6^-$	0.44 <sup>d</sup>	4.2	$T_{\text{M-1}} \approx 200$ K
$\text{NbF}_6^-$	0.58 (Nb)	140	Metallic $\geq 90$ K <sup>e</sup>
$\text{TaF}_6^-$	0.37 (Ta)	21	$T_{\text{M-1}} \approx 140$ K
$\text{I}_3^-$	0.30(I)	7.1	Metallic $\geq 4.2$ K

<sup>a</sup>Determined by energy dispersion spectroscopy from the ratio of sulfur and the elements designated in parentheses. <sup>b</sup>Measured on a single crystal using four-probe method. <sup>c</sup>Contains a solvent (PhCl)<sub>0.22</sub>. <sup>d</sup>Determined by X-ray structure analysis. <sup>e</sup>Cracked at this temperature.

### Electrical transport measurements

Resistivity measurements were performed by a four-probe method along the crystal plane (*//bc* plane) with gold wire and gold paste. High pressure measurements were carried out by using a clamp type cell. The indicated value of applied pressure is 3 kbar less than the pressure applied at room temperature because the pressure is decreased at low temperatures due to the freezing of the daphne oil as pressure medium. Thermoelectric power was measured along the crystal plane as described in the literature.<sup>12</sup>

### Crystal structure determination

The black plate-like crystals of  $\text{AsF}_6^-$  and  $\text{SbF}_6^-$  salts were used for X-ray crystal structure analysis. Crystal and experimental data are shown in Table 2. Data collection and refinement methods are as follows; Rigaku AFC7R diffractometer,  $\omega/2\theta$  mode up to  $2\theta=60^\circ$ ,  $\omega$  scan speed  $16.0$  deg  $\text{min}^{-1}$ , graphite monochromated Mo-K $\alpha$  radiation ( $\lambda=0.71069$  Å). No decay correction was applied. The structure was solved by a direct method (SIR92 for the  $\text{AsF}_6^-$  and SHELXS86 for the  $\text{SbF}_6^-$  salts, respectively).<sup>13</sup> The atomic scattering factors were taken from the International Tables for X-ray Crystallography.<sup>14</sup> Some non-hydrogen atoms (S, As and Sb) were refined anisotropically, while the rest were refined isotropically using full-matrix least-squares methods. The positions of C(18) and C(19) atoms and hydrogen atoms were not refined.

### Band structure calculations

The transfer integrals, band structure and Fermi surface were calculated by a tight-binding method based on the extended Hückel approximation.<sup>15</sup>

### Electron paramagnetic resonance

Electron paramagnetic resonance spectra were measured on a single crystal which was mounted on the cut flat face of a Teflon rod using a small amount of silicon grease and was placed in an evacuated quartz tube. The applied microwave power was 0.1 mW and the modulation field was 10 G.

### Static magnetic susceptibility

Measurements of magnetic susceptibility were carried out on the warming process using a Quantum Design MPMS-2 SQUID magnetometer in field of 1 T. The data were corrected for the diamagnetic contribution estimated from the Pascal's constants ( $\chi^{\text{dia}}=-5.37 \times 10^{-4}$  emu  $\text{mol}^{-1}$  for  $\text{AsF}_6^-$  salt,  $\chi^{\text{dia}}=-5.68 \times 10^{-4}$  emu  $\text{mol}^{-1}$  for  $\text{SbF}_6^-$  salt) and Curie

§Full crystallographic details, excluding structure factors, have been deposited at the Cambridge Crystallographic Data Centre (CCDC). See Information for Authors, *J. Mater. Chem.*, 1998, Issue 1. Any request to the CCDC for this material should quote the full literature citation and the reference number 1145/104.

impurities (0.55 mol% for  $\text{AsF}_6^-$  salt, 0.11 mol% for  $\text{SbF}_6^-$  salt).

## Results and Discussion

### Conducting properties

The electrical properties of CPDTET salts are summarized in Table 1. The tetrahedral  $\text{ClO}_4^-$  salt was a semiconductor with a large activation energy (0.15 eV). In contrast most salts with octahedral ( $\text{AsF}_6^-$ ,  $\text{SbF}_6^-$ ,  $\text{NbF}_6^-$  and  $\text{TaF}_6^-$ ) and linear ( $\text{I}_3^-$ ) anions showed comparatively high conductivity ( $\sigma_{\text{rt}}=10^0\text{--}10^2$  S  $\text{cm}^{-1}$ ), all of which exhibited metallic temperature dependence around room temperature. Exceptionally the  $\text{PF}_6^-$  salt was a semiconductor probably due to a different crystal structure containing a small amount of chlorobenzene which was detected by electron dispersion spectroscopy. The conducting behaviour of the metallic salts is shown in Fig. 1. Among the metallic salts with octahedral anions, the  $\text{AsF}_6^-$  salts displayed metal-like temperature dependence down to 4.2 K though they showed a few resistivity jumps and the resistivity increased a little at low temperature. On the other hand, the  $\text{SbF}_6^-$  and  $\text{TaF}_6^-$  salts exhibited metal-to-semiconductor transitions at 200 and 140 K, respectively. However, their activation energy after the transition is very small ( $\sim 0.002$  eV), indicating the resulting energy gap is tiny. The resistivity of the  $\text{SbF}_6^-$  and  $\text{TaF}_6^-$  salts was measured under applied pressure. The values decreased almost linearly with increasing pressure. The resistivity at 5.3–5.6 kbar was about half of the ambient-pressure value. Furthermore the  $\text{SbF}_6^-$  and  $\text{TaF}_6^-$  salts retained metallic behaviour down to low temperatures under an applied pressure of 5.3–5.6 kbar (Fig. 2). The linear  $\text{I}_3^-$  salt also showed a relatively high conductivity ( $\sigma_{\text{rt}}=7$  S  $\text{cm}^{-1}$ ) and exhibited metallic temperature dependence down to 4.2 K though the resistivity slightly increased at low temperature.

### X-Ray crystal structures of cation radical salts

Among the cation radical salts obtained so far, single crystal X-ray structure analysis was carried out for the  $\text{AsF}_6^-$  and  $\text{SbF}_6^-$  salts. These two salts have the same space group (*Cc*) and are isostructural. There are two crystallographically independent CPDTET molecules (A and B) in a unit cell. On the other hand, one anion is located in a general position. From the population analysis the donor to anion ratio was refined to be 2:0.72 for the  $\text{AsF}_6^-$  salt and 2:0.87 for the  $\text{SbF}_6^-$  salt, indicating an anion site defect.<sup>16</sup> The donor structures and atomic numbering schemes of the  $\text{AsF}_6^-$  salt are shown in

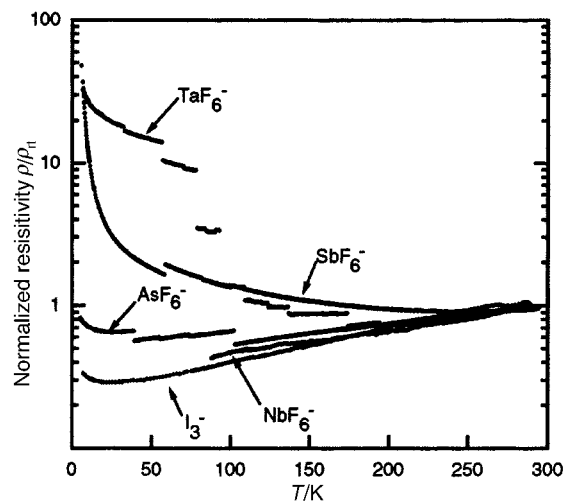


**Fig. 1** Temperature dependence of normalized electrical resistivity of CPDTET salts in the cooling run

**Table 2** Crystallographic data for CPDTET salts

	(CPDTET) <sub>2</sub> (AsF <sub>6</sub> ) <sub>0.72</sub>	(CPDTET) <sub>2</sub> (SbF <sub>6</sub> ) <sub>0.87</sub>
formula	As <sub>0.72</sub> C <sub>28</sub> F <sub>4.32</sub> H <sub>24</sub> S <sub>16</sub>	C <sub>28</sub> F <sub>5.22</sub> H <sub>24</sub> S <sub>16</sub> Sb <sub>0.87</sub>
formula weight	1009.47	1078.55
crystal system	monoclinic	monoclinic
space group	Cc	Cc
Z	4	4
a/Å	40.900(2)	41.17(3)
b/Å	8.192(2)	8.29(2)
c/Å	11.372(2)	11.27(1)
β/Å	99.92(1)	100.0(1)
V/Å <sup>3</sup>	3753(1)	3786(8)
D <sub>calc</sub> /g cm <sup>-3</sup>	1.786	1.892
F(000)	2053.00	2157.40
dimensions/mm <sup>3</sup>	0.36 × 0.30 × 0.02	0.40 × 0.30 × 0.01
μ(MoKα)/cm <sup>-1</sup>	16.25	15.70
ω scan width	1.68 + 0.30 tanθ	1.63 + 0.30 tanθ
reflections measured	5899	5170
unique reflections	5824	5094
reflections used	2406	1809
I/σ(I)	3	2
R <sub>int</sub>	0.022	0.060
R	0.077	0.074
R <sub>w</sub>	0.079	0.081
GOF	3.38	1.47

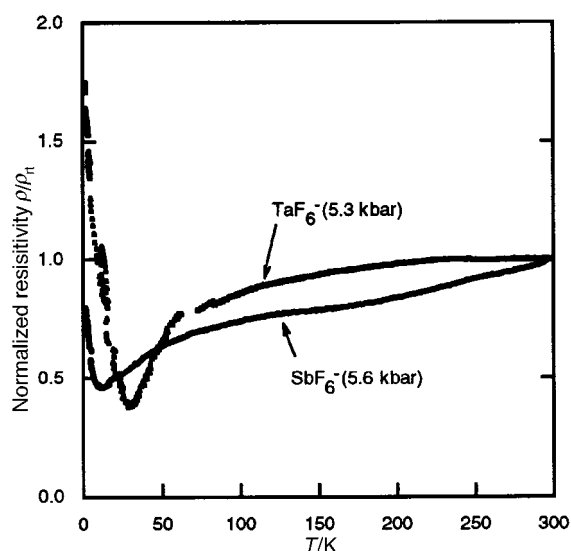


**Fig. 2** Temperature dependence of normalized resistivity of the SbF<sub>6</sub><sup>-</sup> and TaF<sub>6</sub><sup>-</sup> salts under applied pressure

**Fig. 3.** In molecule A, the molecular plane is almost flat, but its cyclopentanylidene ring is bent downwards with a dihedral angle of 9.6° and has a slightly staggered conformation. The C–C bond lengths of the ethylenedithio group are very short [1.35(6) and 1.30(4) Å] compared with the usual C–C single bond length (about 1.51 Å) and the carbon atoms have a large temperature factor, indicating the conformational flexibility of the ethylene bridge. On the other hand, molecule B is also almost planar, but its ethylenedithio ring is bent upwards with a dihedral angle of 9.9° at the S(13)–S(14) position and the cyclopentanylidene ring is slightly twisted. The crystal structure is shown in Fig. 4. Two neighboring donor layers are related to each other with the symmetry operation ( $x + 1/2, y + 1/2, z$ ) in the unit cell, which are separated by the anion sheets [Fig. 4(a)]. All the donors in the crystal are oriented in the same direction. Molecules A and B form a dimer and each dimer is orthogonally arranged in the conducting sheet [(Fig. 4(b)). The donor array of the present salts is classified as the so-called κ-type. Short intermolecular S–S contacts as the so-called κ-type. Short intermolecular S–S contacts (≤3.70 Å) are also indicated in the caption of [Fig. 4(b)]. They exist only between

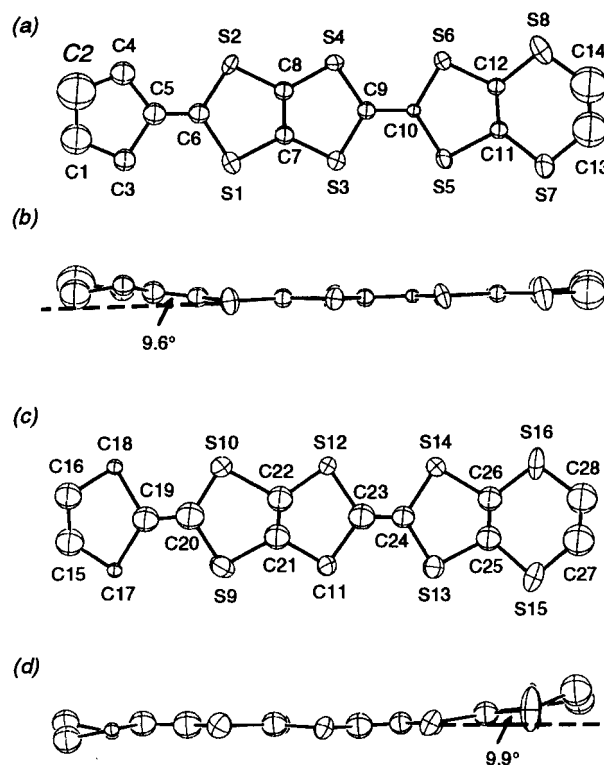


**Fig. 3** ORTEP drawing and atomic numbering scheme of (CPDTET)<sub>2</sub>(AsF<sub>6</sub>)<sub>0.72</sub>: (a) molecule A and (b) side view, (c) molecule B and (d) side view

neighboring dimers as is usually observed in κ-type salts. The shortest distance is 3.36(1) Å. The overlap mode in the dimer is the so-called 'ring-over-bond' type and the interplanar distance within the dimer is 3.60 Å. The slip distance of the TTF skeleton along the molecular long axis is 1.6 Å. Interestingly, the donor molecules A and B are dimerized in a 'head-to-head' manner (Fig. 5) unlike other κ-type salts of unsymmetrical donors like (MeDTET)<sub>3</sub>PF<sub>6</sub>TCE<sub>x</sub><sup>8</sup> (MDT-TTF)<sub>2</sub>AuI<sub>2</sub><sup>3b</sup> and (DMET)<sub>2</sub>AuBr<sub>2</sub><sup>4b</sup> in which two donor molecules are arranged in a 'head-to-tail' manner to avoid the steric hindrance of the flexible ethylenedithio or methylenedithio groups. As mentioned above, the CPDTET molecule has

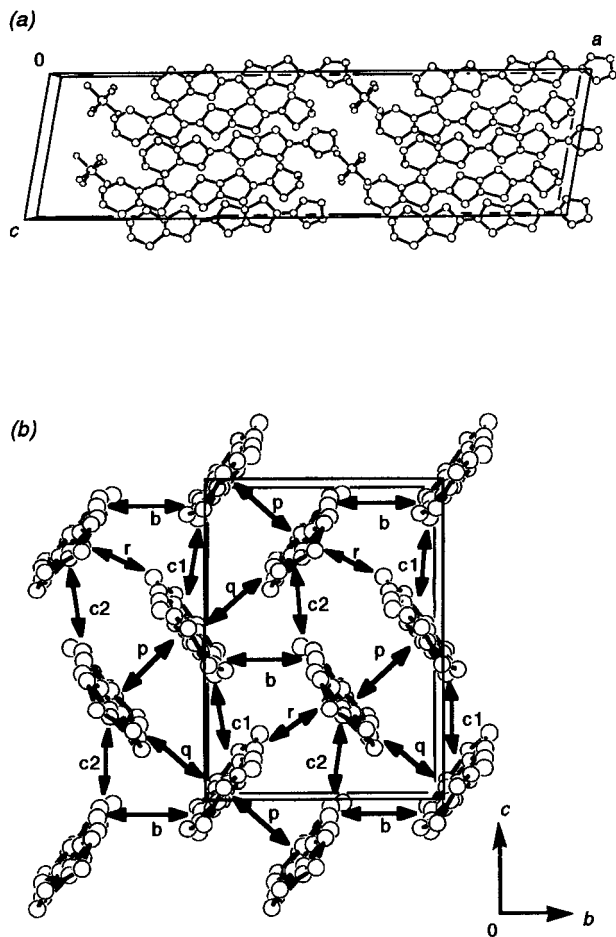


**Fig. 4** Crystal structure of  $(\text{CPDTET})_2(\text{AsF}_6)_{0.72}$  (a) viewed along the  $b$ -axis and (b) viewed along the molecular long axis. Short intermolecular S-S contacts ( $\leq 3.70$  Å):  $b$  S(7)–S(16) 3.386(9) Å;  $c1$  S(5)–S(8) 3.66(1) Å and S(7)–S(8) 3.59(1) Å;  $c2$  S(9)–S(12) 3.69(1) Å and S(15)–S(16) 3.36(1) Å;  $r$  S(8)–S(14) 3.51(1) Å.

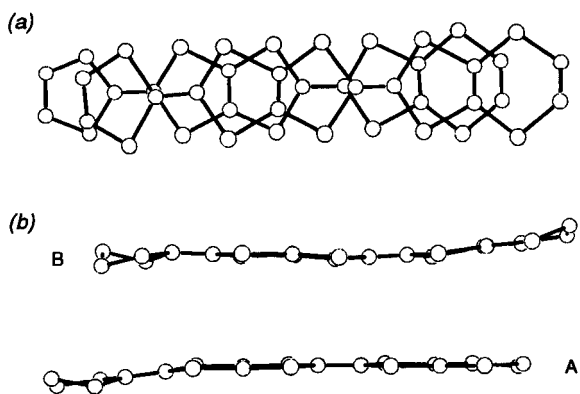


**Fig. 5** Overlap mode in a dimer of  $(\text{CPDTET})_2(\text{AsF}_6)_{0.72}$ : (a) projected onto the molecular plane and (b) the side view

sterically flexible cyclopentanylidene and ethylenedithio groups on both ends of the molecule, in contrast to the case of MeDTET, and the steric hindrance of dimerization is not relieved even if the dimer adopts the head-to-tail arrangement. Therefore we think that CPDTET adopts the head-to-head dimerization mode to increase the effective overlap area of the molecules and to stabilize the electronic state with van der Waals attractive force.

### Electronic band structure and Fermi surface

The dispersion relation and Fermi surfaces of the  $\text{AsF}_6^-$  and  $\text{SbF}_6^-$  salts were calculated by a tight-binding method based on the extended Hückel approximation on a donor layer ( $bc$  plane) [(Fig. 4(b)]. As shown in Table 3, the overlap integrals between molecules arranged parallel to each other ( $p$  and  $b$ ) are two or three times larger than those between molecules perpendicularly arranged ( $q$ ,  $r$ ,  $c1$  and  $c2$ ). Large intradimer overlap integrals ( $p=20.0 \times 10^{-3}$  for the  $\text{AsF}_6^-$  salt and  $p=21.3 \times 10^{-3}$  for the  $\text{SbF}_6^-$  salt) indicate strong dimerization compared with  $(\text{MeDTET})_3\text{PF}_6\text{TCE}_x$  ( $p=13.4 \times 10^{-3}$ ).<sup>8a</sup> In the  $\kappa$ -type CPDTET salts, two donor molecules are dimerized in the 'head-to-head' manner. As a result, the effective overlap area of the TTF skeleton is much wider (about twice) than that of  $\kappa$ -type MeDTET salts in which two donors stack in the 'head-to-tail' manner. Furthermore the calculated coefficients of atomic orbitals of the inner four sulfur atoms in TTF skeleton are two to four times larger than those of the peripheral four sulfur atoms. Therefore these large intradimer overlap integrals of the CPDTET salts are derived from this larger effective overlap area of the TTF skeleton by 'head-to-head' overlap. Because of this strong dimerization, the upper two bands and the lower ones are completely separated (Fig. 6). The energy gap in both the salts is 0.08 eV. The band dispersion is degenerate on the ZM zone boundary as a result of existence of a  $c$ -glide plane. The Fermi surface is essentially a two-dimensional circle but is folded and closed on the ZM boundary similar to the case of  $\kappa$ -(BEDT-TTF)<sub>2</sub>I<sub>3</sub>.<sup>17</sup>

### Thermoelectric power

The measurement of thermoelectric power was carried out for the  $\text{AsF}_6^-$  and  $\text{SbF}_6^-$  salts to clarify the origin of the metal-to-semiconductor transition of the  $\text{SbF}_6^-$  salt. Fig. 7 shows the temperature dependence of thermoelectric power of these salts. The  $\text{AsF}_6^-$  salt exhibited almost  $T$ -linear temperature dependence to zero thermoelectric power, which is characteristic of normal metals. On the other hand, the  $\text{SbF}_6^-$  salt has a very small room temperature thermoelectric power ( $+1.4 \mu\text{V K}^{-1}$ ) compared with that of metallic  $\text{AsF}_6^-$  salt ( $+6.9 \mu\text{V K}^{-1}$ ). These thermoelectric powers are too small for a quarter-

**Table 3** Intermolecular overlap integrals ( $\times 10^{-3}$ ) of  $\kappa$ -type CPDTET salts and  $(\text{MeDTET})_3\text{PF}_6\text{TCE}_x$

	$\text{AsF}_6^-$ salt	$\text{SbF}_6^-$ salt	$(\text{MeDTET})_3\text{PF}_6\text{TCE}_x$
$p$	20.0	21.3	13.4
$b$	13.0	13.7	9.5
$q$	5.0	5.9	4.6
$r$	3.8	2.8	4.6
$c1$	6.6	7.7	6.3
$c2$	4.2	4.3	6.3

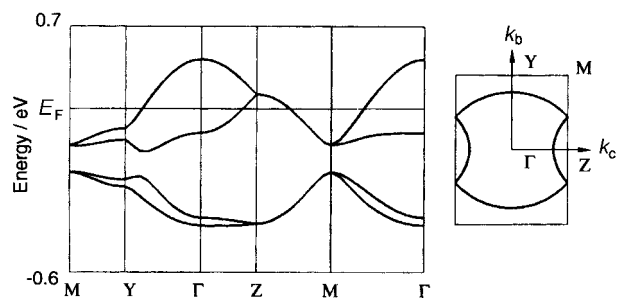


**Fig. 6** Energy band structure and Fermi surface of  $(\text{CPDTET})_2(\text{AsF}_6)_{0.72}$  where  $\Gamma$ , Y, Z and M refer to the reciprocal lattice points  $(0, 0, 0)$ ,  $(0, b^*/2, 0)$ ,  $(0, 0, c^*/2)$  and  $(0, b^*/2, c^*/2)$ , respectively, and  $k_b$  and  $k_c$  are the wave vectors along the  $b^*$  and  $c^*$  axes, respectively

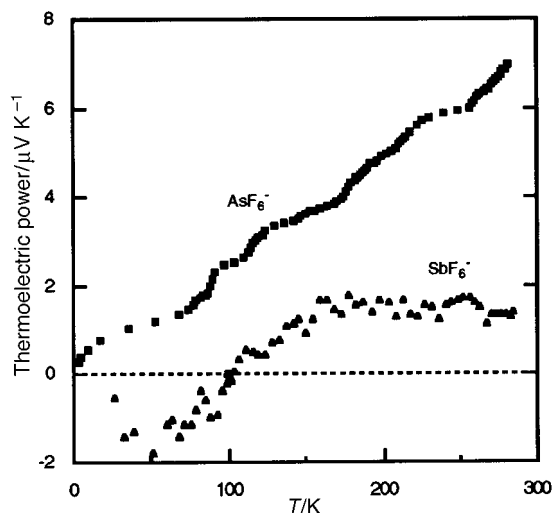


Fig. 7 Temperature dependence of thermoelectric power of the  $\text{AsF}_6^-$  and  $\text{SbF}_6^-$  salts

filled band structure and indicate the band structures of these salts are nearly half-filled and a small amount of positive carriers play a role in the electric conduction. Furthermore the thermoelectric power of the  $\text{SbF}_6^-$  salt showed very weak temperature dependence down to 160 K, and then it decreased  $T$ -linearly and exhibited a small negative value ( $\sim -2 \mu\text{V K}^{-1}$ ) below 100 K, suggesting that the band structure of the  $\text{SbF}_6^-$  salt is very close to half-filled and a small gap opens in the low temperature region.

#### EPR Studies

The angular dependence of the EPR spectra of the new  $\kappa$ -type salt was measured by rotating the crystal in the cavity by use of a goniometer at room temperature. The angular dependence for the  $\text{SbF}_6^-$  salt is shown in Fig. 8. When the static magnetic field was applied parallel to the crystal plane ( $// bc$  plane), the peak-to-peak line width ( $\Delta H_{\text{pp}}$ ) and  $g$ -value show the minimum value (68 G and  $g=2.001$ ). In contrast, they exhibited maximum values (89 G and  $g=2.007$ ) with the magnetic field perpendicular to the conducting plane. At the maximum point the static magnetic field is approximately parallel to the long molecular axis of the donor molecule. These large  $\Delta H_{\text{pp}}$  values are characteristic of the  $\kappa$ -type arrangement of donor molecules.<sup>1c</sup>

Variable temperature EPR measurements have been carried out for the  $\text{AsF}_6^-$  and  $\text{SbF}_6^-$  salts to about 2 K with the

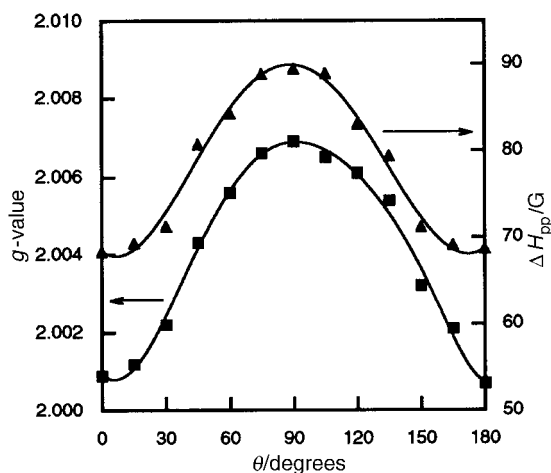


Fig. 8 Angular dependence of peak-to-peak line width ( $\Delta H_{\text{pp}}$ ) and  $g$ -value of the  $\text{SbF}_6^-$  salt

magnetic field approximately perpendicular to the conducting plane. As shown in Fig. 9, the  $\Delta H_{\text{pp}}$  values of these salts are almost constant down to about 150 K and decrease monotonically to 30–40 G below 150 K. In the usual  $\kappa$ -type BEDT-TTF salts, the  $\Delta H_{\text{pp}}$  value increases with decreasing temperature in a metallic region like metallic  $\text{Cu}(\text{NCS})_2^-$ ,  $\text{Cu}(\text{CN})[\text{N}(\text{CN})_2]^-$  and  $\text{Hg}_{2.89}\text{Br}_8^{2-}$  salts.<sup>18</sup> On the other hand, the  $\Delta H_{\text{pp}}$  value decreases with lowering temperature in a semiconducting region when the low-dimensional antiferromagnetic short range order increases like the case of the semiconducting  $\text{Cu}[\text{N}(\text{CN})_2]\text{Cl}^-$  salt.<sup>19</sup> Thus we think that weak antiferromagnetic interaction emerges below room temperature in the  $\kappa$ -type CPDTET salts. The degree of decrease is not so much and an apparent antiferromagnetic transition was not observed. The EPR intensities are estimated from the  $\Delta H_{\text{pp}}$  and amplitude ( $I_m$ ) using the known approximation;  $\text{Intensity} = I_m \times (\Delta H_{\text{pp}})^2$ . The calculated intensities tend to decrease from room temperature with decreasing temperature and also show the existence of a weak antiferromagnetic interaction (Fig. 10). However the data points are very scattered due to the weak and broad line shapes and precise

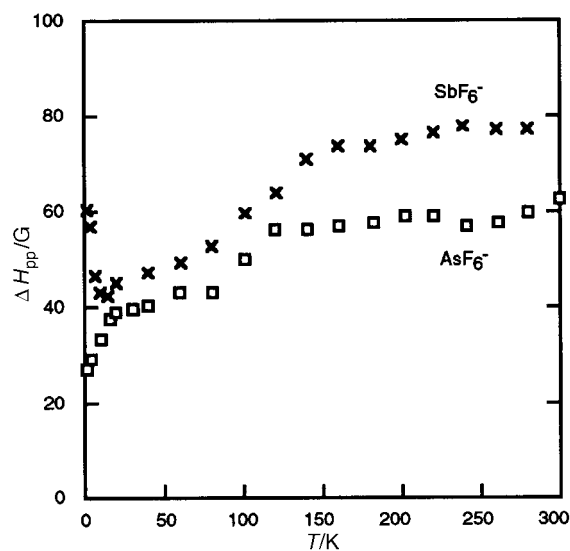


Fig. 9 Temperature dependence of peak-to-peak line width ( $\Delta H_{\text{pp}}$ ) of the  $\text{AsF}_6^-$  and  $\text{SbF}_6^-$  salts

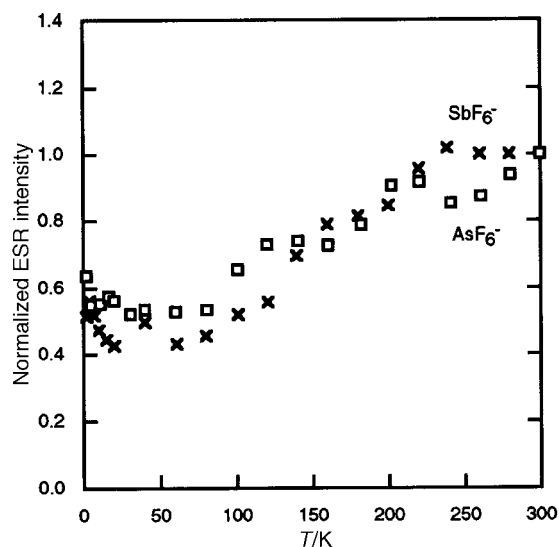


Fig. 10 Temperature dependence of normalized spin susceptibility of the  $\text{AsF}_6^-$  and  $\text{SbF}_6^-$  salts

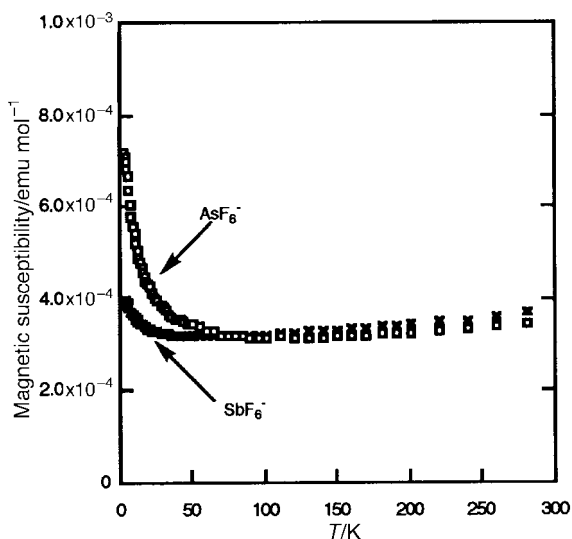


Fig. 11 Temperature dependence of static magnetic susceptibility of the  $\text{AsF}_6^-$  and  $\text{SbF}_6^-$  salts

information about the interaction could not be obtained from the EPR intensities.

#### Static magnetic susceptibilities

The magnetic susceptibilities of the  $\text{AsF}_6^-$  and  $\text{SbF}_6^-$  salts were also measured on a SQUID magnetometer at 1 T because the spin susceptibility of these salts could not be exactly estimated from the EPR measurements due to the weak and broad line shapes. The room temperature susceptibilities are  $3.48 \times 10^{-4} \text{ emu mol}^{-1}$  for the  $\text{AsF}_6^-$  salt and  $3.74 \times 10^{-4} \text{ emu mol}^{-1}$  for the  $\text{SbF}_6^-$  salt after correction for diamagnetic contributions and Curie impurities. These values are close to each other and correspond to that of normal metallic material but the value for the  $\text{SbF}_6^-$  salt is slightly higher than that for the  $\text{AsF}_6^-$  salt. The temperature dependence of these susceptibilities is shown in Fig. 11. They are weakly temperature-dependent, namely, they decrease slightly with decreasing temperature, indicating the weak antiferromagnetic interaction as discussed in the EPR study. The degree of this decrease for the  $\text{SbF}_6^-$  salt is 15% and is higher than that for the  $\text{AsF}_6^-$  salt (10%). These results suggest that these two salts have similar magnetic properties but the  $\text{SbF}_6^-$  salt shows slightly stronger electron correlation and antiferromagnetic interaction than the metallic  $\text{AsF}_6^-$  salt. Though the correction for Curie impurities has been performed, the susceptibilities increase at low temperature. We think that this increase may be derived from the spin localization by lattice defects and this localization seems to cause the slight increase in resistivity of the  $\text{AsF}_6^-$  salt as is shown in Fig. 1.

#### Comparison of $\text{AsF}_6^-$ salt and $\text{SbF}_6^-$ salt

Here we discuss the differences between the  $\text{AsF}_6^-$  and  $\text{SbF}_6^-$  salts. They are isostructural and the donors have a  $\kappa$ -type arrangement in the conducting sheet. From the population analysis there are some defects of the anion site. The electronic structure calculation indicated the upper two bands and lower ones are perfectly separated because of the strongly dimerized structure derived from the head-to-head overlap mode. This situation makes the upper band effectively half-filled and yields a strong electron-correlated system when the donor to anion ratio is 2:1.<sup>20</sup> Though the  $\text{AsF}_6^-$  and  $\text{SbF}_6^-$  salts have the same  $\kappa$ -type crystal structure and similar closed Fermi surface, the transport properties of these two salts are very different; that is, the  $\text{AsF}_6^-$  salt displayed metallic temperature dependence down to 4.2 K, whereas the  $\text{SbF}_6^-$  salt exhibited the

metal-to-semiconductor transition at 200 K. The semiconducting state of the  $\text{SbF}_6^-$  salt had a very small energy gap of 0.002 eV and was suppressed by an applied pressure of 5.6 kbar. The thermoelectric powers of these salts are too small for a quarter-filled band structure and indicate the band structures of these salts are nearly half-filled. The temperature dependence of the thermoelectric powers showed that the  $\text{AsF}_6^-$  salt is a normal metal, but the band structure of the  $\text{SbF}_6^-$  salt is very nearly half-filled and a small gap opens at the low temperature region. On the other hand, the magnetic measurements of these two salts showed similar temperature dependent behaviour of the magnetic susceptibilities and weak antiferromagnetic interaction. So where is the difference between the two salts? All these results are concluded as follows; (1) the band structure of the  $\text{SbF}_6^-$  is very close to half-filled and shows a metal-semiconducting transition due to the strong electron correlation, (2) the  $\text{AsF}_6^-$  salt has a similar crystal structure to the  $\text{SbF}_6^-$  salt and is also affected by the strong electron correlation, but the band filling is far from half-filled because there are more anion defects than in the case of the  $\text{SbF}_6^-$  salt, and so this avoids the semiconducting transition. We think that the electronic states of these two salts are nearly the same and the only difference between the two salts is the occupancy of the anion sites which determines the possibility of the semiconducting transition derived from the strong electron correlation.

#### Conclusion

We have prepared several cation radical salts of the unsymmetrical donor, 2-cyclopentanylidene-1,3-dithiolo[4,5-*d*]-4,5-ethylenedithio-TTF (CPDTET). Most salts showed comparatively high room temperature conductivity and metallic conductive behaviour around room temperature. These results indicate that CPDTET could yield many organic metals stable down to low temperatures. The X-ray crystal structure analysis of the  $\text{AsF}_6^-$  and  $\text{SbF}_6^-$  salts reveals that they have  $\kappa$ -type arrangement in the conducting sheets. It is noted that these salts are the first example of cation radical salts of unsymmetrical donors in which the donors are dimerized in a head-to-head manner. The band calculation indicated the upper two bands and lower ones are completely separated because of the strongly dimerized structure derived from the head-to-head overlap mode. The calculated Fermi surfaces are two-dimensional circles as is often shown by superconducting  $\kappa$ -type BEDT-TTF salts. The measurements of transport and magnetic properties have been performed to discuss the differences between the  $\text{AsF}_6^-$  and  $\text{SbF}_6^-$  salts. We have also discussed the origin of the metal-semiconducting transition of the  $\text{SbF}_6^-$  salt and indicated that the anion content determines the possibility of a semiconducting transition caused by the strong electron correlation. Anyway CPDTET has yielded many metallic salts and shown an unusual crystal structure and interesting physical properties. Thus we think CPDTET would be a suitable donor for researching organic metals in the future.

This work is partially supported by Grants-in-Aid for Scientific Research No. 06243215, 07232219, and 00063275 from the Ministry of Education, Science, and Culture of Japan. One of the authors (H. F.) is indebted to the JSPS Research Fellowships for Young Scientists.

#### References

- (a) T. Ishiguro and K. Yamaji, *Organic Superconductors*, Springer-Verlag, Berlin, Heidelberg, 1990; (b) *The Physics and Chemistry of Organic Superconductors*, ed. G. Saito and S. Kagoshima, Springer-Verlag, Berlin, Heidelberg, 1990; (c) J. M. Williams, J. R. Ferraro, R. J. Thorn, K. D. Carlson, U. Geiser, H. H. Wang, A. M. Kini and M.-H. Whangbo, *Organic Superconductors*, Prentice Hall, New Jersey, 1992.

- 2 Recent Proceedings of International Conferences: (a) *Synth. Met.*, 1995, **69–71**, ed. Y. W. Park and H. Lee; (b) *Synth. Met.*, 1997, **84–86**, ed. Z. V. Vardeny and A. J. Epstein.
- 3 (a) G. C. Papavassiliou, G. A. Mousdis, J. S. Zambounis, A. Terzis, A. Hountas, B. Hilti, C. W. Mayer and J. Pfeiffer, *Synth. Met.*, 1988, **27**, B379; (b) A. M. Kini, M. A. Beno, D. Son, H. H. Wang, K. D. Carlson, L. C. Porter, U. Welp, B. A. Vogt, J. M. Williams, D. Jung, M. Evain, M.-H. Whangbo, D. L. Overmyer and J. E. Schirber, *Solid State Commun.*, 1989, **69**, 503.
- 4 (a) K. Kikuchi, M. Kikuchi, T. Namiki, K. Saito, I. Ikemoto, K. Murata, T. Ishiguro and K. Kobayashi, *Chem. Lett.*, 1987, 931; (b) K. Kikuchi, Y. Honda, Y. Ishikawa, K. Saito, I. Ikemoto, K. Murata, H. Anzai and T. Ishiguro, *Solid State Commun.*, 1988, **66**, 405.
- 5 Y. Misaki, H. Nishikawa, K. Kawakami, T. Uehara and T. Yamabe, *Tetrahedron Lett.*, 1992, **33**, 4321.
- 6 (a) Y. Misaki, H. Nishikawa, H. Fujiwara, K. Kawakami, T. Yamabe, H. Yamochi and G. Saito, *J. Chem. Soc., Chem. Commun.*, 1992, 1408; (b) Y. Misaki, K. Kawakami, H. Nishikawa, H. Fujiwara, T. Yamabe and M. Shiro, *Chem. Lett.*, 1993, 445.
- 7 S. Aonuma, Y. Okano, H. Sawa, R. Kato and H. Kobayashi, *J. Chem. Soc., Chem. Commun.*, 1992, 1193.
- 8 (a) Y. Misaki, H. Nishikawa, T. Yamabe, T. Mori, H. Inokuchi, H. Mori and S. Tanaka, *Chem. Lett.*, 1993, 1341; (b) Y. Misaki, H. Nishikawa, H. Fujiwara, T. Yamabe, T. Mori, H. Mori and S. Tanaka, *Synth. Met.*, 1995, **70**, 1151.
- 9 (a) G. Saito, *Phosphorus, Sulfur and Silicon*, 1992, **67**, 345; (b) H. Yamochi, T. Komatsu, N. Matsukawa, G. Saito, T. Mori, M. Kusunoki and K. Sakaguchi, *J. Am. Chem. Soc.*, 1993, **115**, 11 319.
- 10 Preliminary proceeding: H. Fujiwara, T. Miura, Y. Misaki, T. Yamabe, T. Mori, H. Mori and S. Tanaka, *Mol. Cryst. Liq. Cryst.*, 1996, **284**, 329.
- 11 H. Anzai, J. M. Delrieu, S. Takasaki, S. Nakatsuji and J. Yamada, *J. Cryst. Growth*, 1995, **154**, 145.
- 12 T. Mori, H. Inokuchi, A. Kobayashi, R. Kato and H. Kobayashi, *Phys. Rev. B*, 1988, **38**, 5913.
- 13 (a) A. Altomare, M. C. Burla, M. Camalli, M. Cascarano, C. Giacovazzo, A. Guagliardi, G. Polidori, *J. Appl. Crystallogr.*, 1994, **27**, 432; (b) G. M. Sheldrick, in *Crystallographic Computing 3*, Oxford University Press, 1985, p. 175.
- 14 D. T. Cromer and J. T. Waber, *International Tables for X-ray Crystallography*, vol. 4, Kynoch Press, Birmingham, 1974.
- 15 T. Mori, A. Kobayashi, Y. Sasaki, H. Kobayashi, G. Saito and H. Inokuchi, *Bull. Chem. Soc. Jpn.*, 1984, **57**, 627.
- 16 The final *R* value is much lower than that of the 2:1 assumption for the AsF<sub>6</sub><sup>-</sup> salt (0.092 to 0.077) and for the SbF<sub>6</sub><sup>-</sup> salt (0.081 to 0.074).
- 17 D. Jung, M. Evain, J. J. Novoa, M.-H. Whangbo, M. A. Beno, A. M. Kini, A. J. Schultz, J. M. Williams and P. J. Nigrey, *Inorg. Chem.* 1989, **28**, 4516.
- 18 (a) H. Urayama, H. Yamochi, G. Saito, S. Sato, T. Sugano, M. Kinoshita, A. Kawamoto, J. Tanaka, T. Inabe, T. Mori, Y. Maruyama, H. Inokuchi and K. Oshima, *Synth. Met.*, 1988, **27**, A393; (b) H. H. Wang, B. A. Vogt, U. Geiser, M. A. Beno, K. D. Carlson, S. Kleinjan, H. Thorup and J. M. Williams, *Mol. Cryst. Liq. Cryst.*, 1990, **181**, 135.
- 19 M. Kubota, G. Saito, H. Ito, T. Ishiguro and N. Kojima, *Mol. Cryst. Liq. Cryst.*, 1996, **284**, 367.
- 20 T. Komatsu, N. Matsukawa, T. Inoue and G. Saito, *J. Phys. Soc. Jpn.*, 1996, **65**, 1340.

Paper 8/01375F; Received 17th February, 1998